Technical Physics, Vol. 47, No. 4, 2002, pp. 470–473. Translated from Zhurnal Tekhnicheskoĭ Fiziki, Vol. 72, No. 4, 2002, pp. 99–102.

EXPERIMENTAL INSTRUMENTS AND TECHNIQUES

High-Frequency Dielectric Spectra from Liquid Crystals of Series *n*CB and *n*OCB

B. A. Belyaev, N. A. Drokin, V. F. Shabanov, and V. N. Shepov

Kirenskiĭ Institute of Physics, Siberian Division, Russian Academy of Sciences, Akademgorodok, Krasnoyarsk, 660036 Russia

e-mail: belyaev@iph.krasn.ru

Received July 5, 2001

Abstract—The design of a resonant frequency-tunable high-sensitivity microstrip sensor is suggested. The permittivity dispersion of liquid crystals of two homologic series, alkylcyanobiphenyls (7CB and 8CB) and alkyloxycyanobiphenyls (7OCB and 8OCB), is studied at frequencies of 100–900 MHz. The dielectric spectra are shown to be the sum of the Debye relaxation and dielectric resonances observed at $f \approx 160$, 280, 360, 450, 550, and 650 MHz. The dielectric resonances are present in the spectra of all the samples in both the nematic and isotropic phase. The substitution of an oxygen atom (series *n*OCB) for a carbon atom (series *n*CB) in liquid crystal molecules has a minor effect on the dielectric resonance frequencies but changes the resonance intensities and splits some of the resonance lines. © *2002 MAIK "Nauka/Interperiodica".*

INTRODUCTION

The Cole–Cole diagrams are very suitable for evaluating the deviation of liquid crystal dielectric spectra from the Debye frequency dependence of the dielectric constants [1, 2]. This requires measurements to be made at several widely separated frequencies in the high-frequency and microwave ranges. The deviations are usually described by a set of Debye relaxation regions. However, because of the lack of adequate experimental data, the reason for a number of spectral features remains unclear. In [3], the dielectric spectra in a wide frequency range (100 kHz–10 GHz) were studied by time-domain spectroscopy. It was shown that the dielectric spectrum taken from liquid crystals of the *n*CB series shows individual faint non-Debye dispersion regions at frequencies of 39, 225, and 550 MHz for 7CB and 34.3, 225, and 600 MHz for 8CB. It is of interest that these regions are observed in both the mesomorphic state and the isotropic phase.

The existence of extra low-intensity narrow-band dispersion regions was also reported in [4], where the dielectric spectra of liquid crystals placed in porous media were studied. In that work, the dispersion features of 5CB and 8CB crystals were observed for the perpendicular component of the permittivity in the nematic phase at 100 MHz.

In [5], the dispersion region of the permittivity was studied in *n*CB liquid crystals at frequencies from 50 to 500 MHz with special microstrip resonant sensors. Distinct extra dispersion regions imposed on the conventional Debye relaxation pattern were found. It is worthy to note that the frequency of the most intense region at 300 MHz does not depend on a specific representative from this homologic series, as well as on temperature and type of liquid-crystal ordering (nematic or smectic). At the same time, the intensity of this extra region strongly varies with temperature and homologic type.

In this work, we further refine the method of measuring the dielectric dispersion with microstrip resonant sensors and study the dielectric spectra of two types of liquid crystals: *n*-alkylcyanobiphenyls (7CB and 8CB) and *n*-alkyloxycyanobiphenyls (7OCB and 8OCB) at frequencies from 100 to 900 MHz. Also, we compare these spectra and discuss the effect of oxygen (*n*OCB series), which substitutes carbon (*n*CB series) in liquid crystal molecules, on the relaxation and resonance characteristics of the dielectric spectra.

MICROSTRIP INSTRUMENT SENSOR AND EXPERIMENTAL METHODS

High-sensitivity frequency-tunable (in discrete steps) resonance sensors built around microstrip structures have proved themselves a promising tool for measuring the dispersion in the decimeter range [6]. Such sensors operate with small amounts (volumes) of materials tested and take the dielectric spectra by measuring the real and imaginary components of the permittivity with a small frequency step.

For taking the dielectric spectra from the liquid crystals, we used the modified design of the microstrip resonant sensor [6] (Fig. 1). The sensor substrate is a 15×30-mm alumina plate with a permittivity $\varepsilon = 9.6$ and a thickness $h = 1$ mm. The lower plated side of the substrate is soldered to the metallic base of the sensor, which serves as a screen. On the upper side of the substrate, microstrip conductors forming a half-wave rectangular microstrip resonant loop are patterned by chemical etching. Input and output microstrip lines

1063-7842/02/4704-0470$22.00

(*A* and *B*) are connected to the opposite sides of this loop through coupling capacitors C_c. A capacitive measuring interdigitation C_x with a spacing of 0.15 mm is placed at the antinode of the microwave field of the resonator. Three breaks to connect lumped elements controlling the operation of the sensor were etched in the microstrip conductor at the maximum of the microwave field. The resonant frequency of the sensor can be varied in wide limits. This is achieved by inserting either calibrated inductances *L*, which lower the frequency of the sensor, or an electrically controlled capacitor (varactor *V*), which raises the frequency, into the central break of the microstrip conductor. In this way, the frequency of the sensor can be increased from 100 to 900 MHz in 20 MHz steps. The capacitors C_1 and C_2 and resistors R_1–R_4 serve to isolate the controlling circuits and to apply a dc orienting electric field to the sample. In the nematic phase, the long axis of the molecules rotate toward the microwave field when a voltage of ≈25 V is applied to the sample. In this case, the longitudinal component $\varepsilon_{\parallel}(f)$ of the permittivity is measured. The transverse component $\varepsilon_{\perp}(f)$ is measured by applying a permanent magnetic field H = 2500 Oe perpendicularly to the microwave electric field.

A 0.20-mm-thick liquid crystal sample was placed directly on the interdigitation, which was bounded by a glass rim, and covered by a Teflon film to prevent contamination. Identical expendable measuring cells were made for either liquid crystal homologue by a specially developed precise lithography technique that offers high reproducibility. The cells were connected to the mutual resonance loop. Such an approach provides a quick replacement of the samples and also prevents them from being contaminated during measurements, which inevitably occurs when a single measuring cell is used.

The real component of the permittivity was calculated from the difference in the resonance frequencies of the sensors with and without the sample. The imaginary component was calculated from the change in the loaded *Q* factor of the resonator when the liquid crystal was placed in it. The amplitude–frequency responses of the microstrip sensors were recorded with an R4-37 automated meter of complex transfer coefficients. For the nematic samples, the cell temperature was kept at $T = (T_{n-i} - 4)$ K, where T_{n-i} is the temperature of the nematic-to-isotropic phase transition, for their dielectric spectra to be convenient to compare. For the samples in the isotropic phase, the temperature was kept at $T = (T_{n-i} + 4)$ K. The absolute accuracy of temperature maintenance was $\Delta T = \pm 0.1$ K or higher.

RESULTS

Along with taking the high-frequency spectra, we measured the permittivity at some frequencies in the megahertz range. It was necessary for providing the desired accuracy in numerically approximating the frequency dependence of the permittivity with the Debye relaxation formula. By way of example, Fig. 2 demonstrates the dielectric spectrum $\varepsilon'_{\parallel}(f)$ for the 7CB sample. The inset here shows the Cole–Cole diagram with data points. In the right-hand side of this diagram, the data points are fairly well described by a semicircle. In the left-hand side, however, the measurements markedly deviate from the semi-circle both to the left and to the right. As follows from the dispersion curve $\varepsilon'_{\parallel}(f)$ in Fig. 2, such a deviation occurs because the dielectric spectrum contains faint yet well distinguishable non-Debye dispersion regions at $f > 100$ MHz.

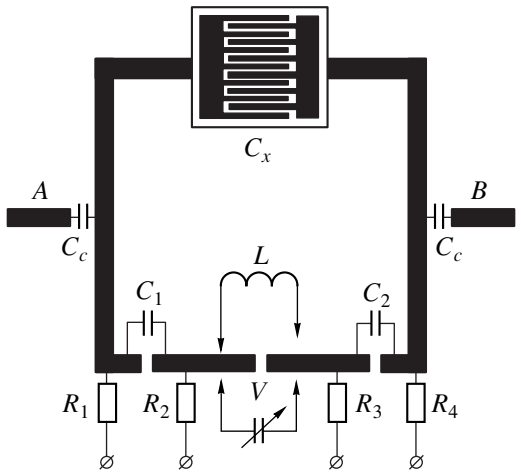

Fig. 1. Microstrip resonant sensor.

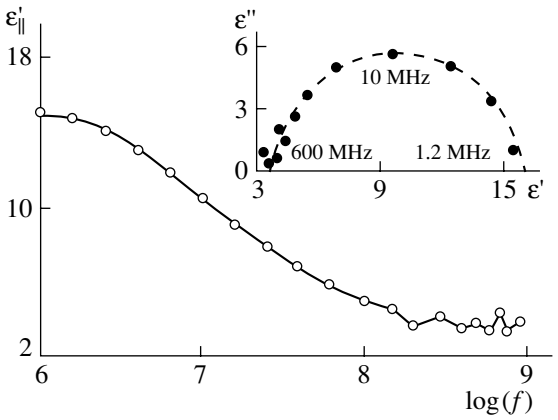

Fig. 2. Frequency dependence of $\varepsilon'_{\parallel}(f)$ in semilogarithmical coordinates for 7CB. The inset shows the Cole–Cole diagram.

Figure 3 shows the high-frequency part of the dielectric spectrum for the real, $\varepsilon'_{\parallel}(f)$, and imaginary, $\varepsilon''_{\parallel}(f)$, components of the permittivity of the 7CB liquid crystal sample. The dashed curve corresponds to the Debye approximation of $\varepsilon'_{\parallel}(f)$ with a single relaxation

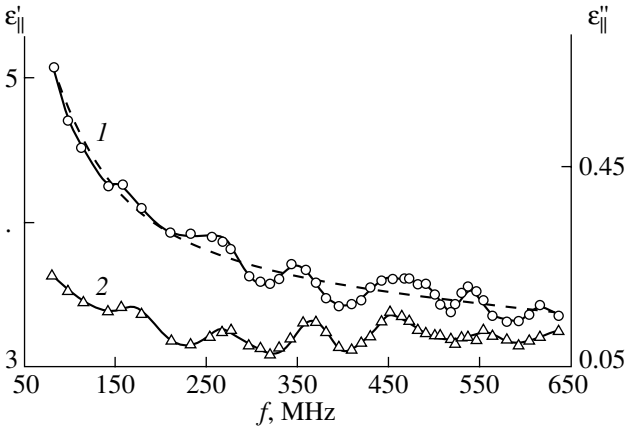

Fig. 3. High-frequency spectra (*1*) $\varepsilon'_{\parallel}(f)$ and (*2*) $\varepsilon''_{\parallel}(f)$ for 7CB sample.

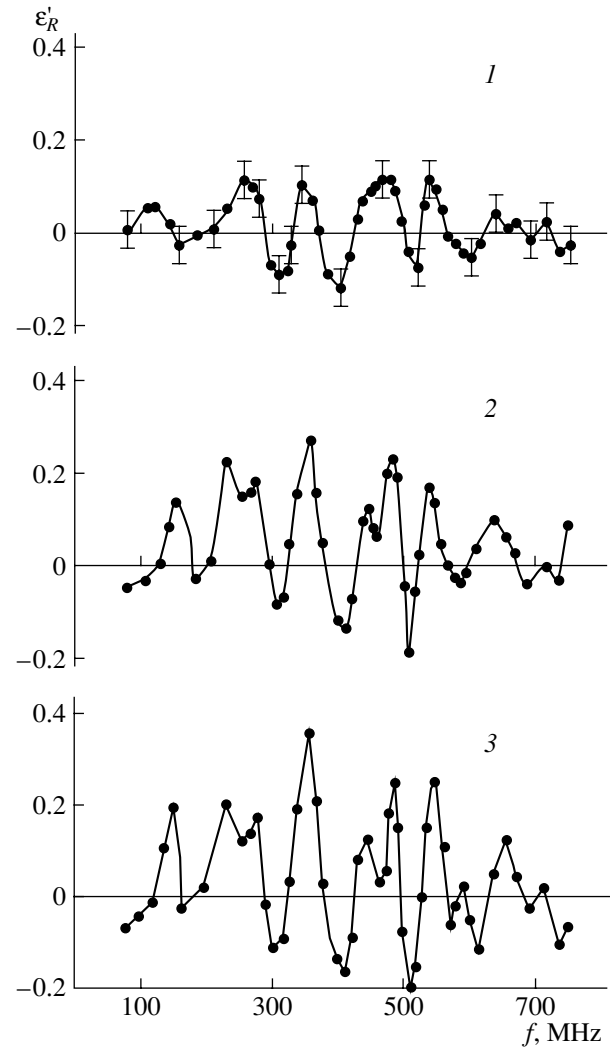

Fig. 4. Resonance spectra ε'_R obtained from $\varepsilon'_{\parallel}(f)$ for (*1*) 7CB, (*2*) 7OCB, and (*3*) 8OCB samples.

time $\tau = 3.25 \times 10^{-8}$ s. The extra dispersion regions with $\varepsilon''_{\parallel}(f)$ peaks at $f \approx 160$, 280, 360, 450, 550, and 650 MHz. Several hardly distinguishable peaks at higher frequencies up to 900 MHz are also observed. Comparing curves *1* and *2*, one can see that the peaks of $\varepsilon''_{\parallel}(f)$ in Fig. 3 coincide with the points where the dispersion curve $\varepsilon'_{\parallel}(f)$ meets the dashed curve, which corresponds to the Debye approximation. With the narrow extra dispersion regions, such behavior of $\varepsilon'_{\parallel}(f)$ and $\varepsilon''_{\parallel}(f)$ is typical of resonance processes. These may be microwave-field-induced intramolecular vibrations of mobile molecular fragments. A phenomenological dielectric spectrum can be described by the sum of the Debye relaxation and dielectric resonances:

$$\varepsilon'(\omega) - \varepsilon'_{\infty} = \frac{(\varepsilon'_0 - \varepsilon'_{\infty})}{1 + \omega^2\tau^2} + \frac{1}{2}\sum_i \Delta\varepsilon_i \times \left[\frac{1 + \omega_{0i}(\omega + \omega_{0i})g_i^2}{1 + (\omega + \omega_{0i})^2 g_i^2} + \frac{1 - \omega_{0i}(\omega - \omega_{0i})g_i^2}{1 + (\omega - \omega_{0i})^2 g_i^2}\right], \quad (1)$$

where ε'_0 and ε'_{∞} are the real components of the static and high-frequency permittivities, $\tau = 1/2\pi f_D$ is the relaxation time (f_D is the Debye resonance frequency), $\Delta\varepsilon$ is the resonance intensity, ω_0 is the resonance frequency, g is the damping factor, i is the resonance number, and $\omega = 2\pi f$.

For more detailed comparison of the frequencies and heights of the resonance peaks, we proceeded as follows. From the spectrum $\varepsilon'_{\parallel}(f)$ measured, the numerically approximated Debye relaxation contribution was subtracted. The "resonance spectra" $\varepsilon'_R(f)$ thus calculated for the 7CB, 7OCB, and 8OCB samples are given in Fig. 4 for the nematic phase. Even slight distortions of the lines are discovered, and the behavior of the resonance frequencies and peak intensities is clearly seen. Note that the resonance spectrum for 8CB differs from that for 7CB insignificantly and is omitted in Fig. 4. It follows from the spectra that the typical resonance frequencies determined from Fig. 3 ($f \approx 160$, 280, 360, 450, 550, and 650 MHz) do not depend on the mesogene type for both *n*CB and *n*OCB series. However, the presence of oxygen in an alkyloxycyanobiphenyl molecule (7OCB and 8OCB) between the rigid core and loose H–C–H alkyl groups increases the intensity of the resonance peaks and even causes some of them to split.

In the isotropic phase, the shape of the spectra remains virtually unchanged for both series, but the resonance line intensity increases almost twice. Such behavior was also observed in [5, 7] for 5CB and 6CB samples. Comparing the Debye relaxation parameters obtained by approximation, one can see that the substi-

tution of an oxygen atom for a carbon atom in liquid crystal molecules strongly affects the Debye parameters: the relaxation time decreases, the high-frequency component $\varepsilon'_{\parallel}(\infty)$ of the permittivity grows, and the dielectric anisotropy increases. The numerical values of these parameters for the liquid crystals studied are very close to those obtained in [1, 2, 8].

It was shown [8] that an angle β between the dipole moment of an alkyl group and the axis of symmetry of the molecule increases with *n* in the *n*CB series and still stronger in the *n*OCB series. In other words, as the length of alkyl groups in the *n*CB and *n*OCB series increases, so does the normal component of the total dipole moment of the molecules. It seems likely that the change in the resonance line intensity and the split of the lines are also associated with an increase in the normal component of the dipole moment of the molecules. Of course, this assumption needs experimental verification; however, it should be taken into account in studying the dielectric spectra considered in this work.

CONCLUSION

With special microstrip frequency-tunable resonant sensors, we studied the high-frequency dielectric spectra of alkylcyanobiphenyl (7CB and 8CB) and alkyloxycyanobiphenyl (7OCB and 8OCB) liquid crystals at frequencies between 100 and 900 MHz. The dielectric spectra of each of the crystals are described by the sum of the Debye relaxation and dielectric resonances at $f \approx$ 160, 280, 360, 450, 550, and 650 MHz. For the longitudinal component $\varepsilon'_{\parallel}(f)$ of the permittivity, the relaxation is characterized by a single relaxation time for each of the crystals. By comparing the dielectric spectra, we conclude that oxygen in the *n*OCB liquid crystals has a minor effect on the dielectric resonance frequencies but changes the resonance intensities and causes some of the resonance line to split.

ACKNOWLEDGMENTS

This work was supported by the Russian Foundation for Basic Research (grant no. 00-03-32206).

Shepov greatly appreciates the financial support from the expert group in the young scientist competition (Siberian Division, Russian Academy of Sciences) devoted to Akademician Lavrent'ev's 100th birthday.

REFERENCES

1. D. Lippens, J. P. Parneix, and A. Chapoton, J. Phys. (Paris) **38**, 1465 (1977).
2. J. M. Wacrenier, C. Druon, and D. Lippens, Mol. Phys. **43**, 97 (1981).
3. T. K. Bose, B. Campbell, S. Yagihara, and J. Thoen, Phys. Rev. A **36**, 5767 (1987).
4. G. P. Sinha and F. M. Aliev, Phys. Rev. E **58**, 2001 (1998).
5. B. A. Belyaev, N. A. Drokin, V. F. Shabanov, and V. N. Shepov, Fiz. Tverd. Tela (St. Petersburg) **42**, 956 (2000) [Phys. Solid State **42**, 987 (2000)].
6. B. A. Belyaev, N. A. Drokin, and V. N. Shepov, Zh. Tekh. Fiz. **65** (2), 189 (1995) [Tech. Phys. **40**, 216 (1995)].
7. B. A. Belyaev, N. A. Drokin, V. F. Shabanov, and V. N. Shepov, Pis'ma Zh. Éksp. Teor. Fiz. **66**, 251 (1997) [JETP Lett. **66**, 271 (1997)].
8. S. Urban, B. Gestblom, and A. Wurflinger, Mol. Cryst. Liq. Cryst. **331**, 1973 (1999).

Translated by V. Isaakyan